ORIGINAL RESEARCH

Enhanced delivery of paclitaxel liposomes using focused ultrasound with microbubbles for treating nude mice bearing intracranial glioblastoma xenografts

Yuanyuan Shen,[1] Zhaoke Pi,[1]
Fei Yan,[2] Chih-Kuang Yeh,[3]
Xiaojun Zeng,[4] Xianfen Diao,[1]
Yaxin Hu,[1] Siping Chen,[1] Xin
Chen,[1] Hairong Zheng[2]

[1]National-Regional Key Technology
Engineering Laboratory for Medical
Ultrasound, Guangdong Key Laboratory for
Biomedical Measurements and Ultrasound
Imaging, School of Biomedical Engineering,
Health Science Center, Shenzhen University,
Shenzhen, People's Republic of China;
[2]Paul C Lauterbur Research Center for
Biomedical Imaging, Institute of Biomedical
and Health Engineering, Shenzhen Institutes
of Advanced Technology, Chinese Academy
of Sciences, Shenzhen, People's Republic
of China; [3]Department of Biomedical
Engineering and Environmental Sciences,
National Tsing Hua University, Hsinchu,
Taiwan; [4]Shenzhen Second People's
Hospital, Shenzhen, People's Republic
of China

Correspondence: Xin Chen
National-Regional Key Technology Engineering
Laboratory for Medical Ultrasound, Guangdong
Key Laboratory for Biomedical Measurements
and Ultrasound Imaging, School of Biomedical
Engineering, Health Science Center, Shenzhen
University, 3688 Nanhai Avenue, Shenzhen
518060, People's Republic of China
Tel +86 755 8667 4605
Fax +86 755 8667 1920
Email chenxin@szu.edu.cn

Fei Yan
Paul C Lauterbur Research Center for
Biomedical Imaging, Institute of Biomedical
and Health Engineering, Shenzhen Institutes
of Advanced Technology, Chinese Academy
of Sciences, 1068 Xueyuan Avenue, Shenzhen
University Town, Shenzhen, 518055, People's
Republic of China
Tel +86 755 8639 2284
Fax +86 755 9638 2299
Email fei.yan@siat.ac.cn

Abstract: Paclitaxel liposomes (PTX-LIPO) are a clinically promising antineoplastic drug formulation for the treatment of various extracranial cancers, excluding glioblastoma. A main reason for this is the presence of the blood–brain barrier (BBB) or blood–tumor barrier (BTB), preventing liposomal drugs from crossing at a therapeutically meaningful level. Focused ultrasound (FUS) in conjunction with microbubbles (MBs) has been suggested in many studies to be an effective approach to increase the BBB or BTB permeability. In this study, we investigated the feasibility of enhancing the delivery of PTX-LIPO in intracranial glioblastoma-bearing nude mice using pulsed low-intensity FUS exposure in the presence of MBs. Our results showed that the delivery efficiency of PTX-LIPO could be effectively improved in terms of the penetration of both the BBB in vitro and BTB in vivo by pulsed FUS sonication with a 10 ms pulse length and 1 Hz pulse repetition frequency at 0.64 MPa peak-rarefactional pressure in the presence of MBs. Quantitative analysis showed that a 2-fold higher drug concentration had accumulated in the glioblastoma 3 h after FUS treatment, with 7.20 ± 1.18 µg PTX per g glioma tissue. Longitudinal magnetic resonance imaging analysis illustrated that the intracranial glioblastoma progression in nude mice treated with PTX-LIPO delivered via FUS with MBs was suppressed consistently for 4 weeks compared to the untreated group. The medium survival time of these tumor-bearing nude mice was significantly prolonged by 20.8%, compared to the untreated nude mice. Immunohistochemical analysis further confirmed the antiproliferation effect and cell apoptosis induction. Our study demonstrated that noninvasive low-intensity FUS with MBs can be used as an effective approach to deliver PTX-LIPO in order to improve their chemotherapy efficacy toward glioblastoma.

Keywords: paclitaxel liposomes, focused ultrasound, microbubbles, blood-brain barrier

Introduction

Glioblastoma multiforme (GBM) is the most common and aggressive primary malignant brain tumor and is characterized by high recurrence and poor prognosis. The median survival time of GBM patients is only 12–15 months, with <5% of patients surviving longer than 5 years, even after treatments.[1] Chemotherapy is an important treatment modality after surgery for suppressing the disease. However, the existence of the blood–tumor barrier (BTB) hampers extravasation of most therapeutic agents from the blood to the brain tumor tissue, thus representing a major challenge to effective chemotherapy.[2] Although the integrity of the BTB is often partially compromised in the glioma center, the permeability is highly heterogeneous; in particular, the BTB

remains intact in the tumor margin where GBM cells often infiltrate. The presence of intact BTB in these regions of tumors considerably impedes drug delivery from the blood to the tumor tissue, leading to a high recurrence rate after chemotherapy.[3]

A host of animal studies in recent years have demonstrated that in the presence of circulating microbubbles (MBs), focused ultrasound (FUS) at low acoustic pressures could be used to open the blood–brain barrier (BBB) of normal brains locally, noninvasively and reversibly.[4–9] Studies performed on nonhuman primates have revealed that BBB opening could be realized by FUS exposure with MBs through the intact skull. The study of McDannold et al showed that repeated and reversible BBB disruption could be achieved in rhesus macaques using 220 kHz FUS at 0.15 MPa without any evident histologic or functional damage.[10] It was also demonstrated that the BBB in a targeted region was opened safely in two male rhesus monkeys using a single-element 500 kHz spherical transducer ultrasound system with real-time cavitation monitoring.[7] All these studies have provided support for the potential feasibility of this unique noninvasive approach toward the drug delivery of chemotherapeutic agents for the treatment of central nervous system diseases.

Paclitaxel (PTX) is a drug that is clinically effective against a wide range of extracranial cancers. Notably, nanoparticle carrier systems have been under development to formulate PTX owing to its extremely lipophilic nature.[11] Among these alternative delivery systems, liposomes are capable of encapsulating hydrophobic drugs to minimize their detrimental toxicities while also enhancing their therapeutic efficacy.[12,13] Nonetheless, the delivery efficiency of PTX liposomes (PTX-LIPO) has been quite limited by the obstacle of the BTB. There have been several experimental studies performed on brain tumor models to explore the delivery outcome or therapeutic efficacy of doxorubicin (DOX)-loaded liposomes delivered using FUS in conjunction with MBs. The results showed increased DOX accumulation in the brain tumor tissue and improved survival time of tumor-bearing animals, indicating that FUS with MBs may provide an attractive modality to enhance the penetration of other liposomal anticancer drugs that are impeded by the BTB, thus ameliorating their chemotherapeutic efficacy.[14–16] To the best of our knowledge, no study on the delivery of PTX-LIPO mediated by noninvasive FUS with MBs or their therapeutic effect on GBM has yet been reported.

The main purpose of this study was to explore the feasibility of enhancing the PTX-LIPO delivery outcome using FUS exposure in conjunction with MBs on an intracranial glioblastoma nude mice model (Figure 1). The permeability of the BBB subjected to FUS with MBs was first studied in a BBB-mimetic bEnd.3 monolayer model in vitro. Then, the enhanced delivery of PTX induced by this method was evaluated in nude mice bearing intracranial U87 MG human glioblastoma. The biodistribution of PTX in organs and glioma was studied quantitatively. The in vivo therapeutic efficacy, tumor proliferation and apoptosis were also investigated.
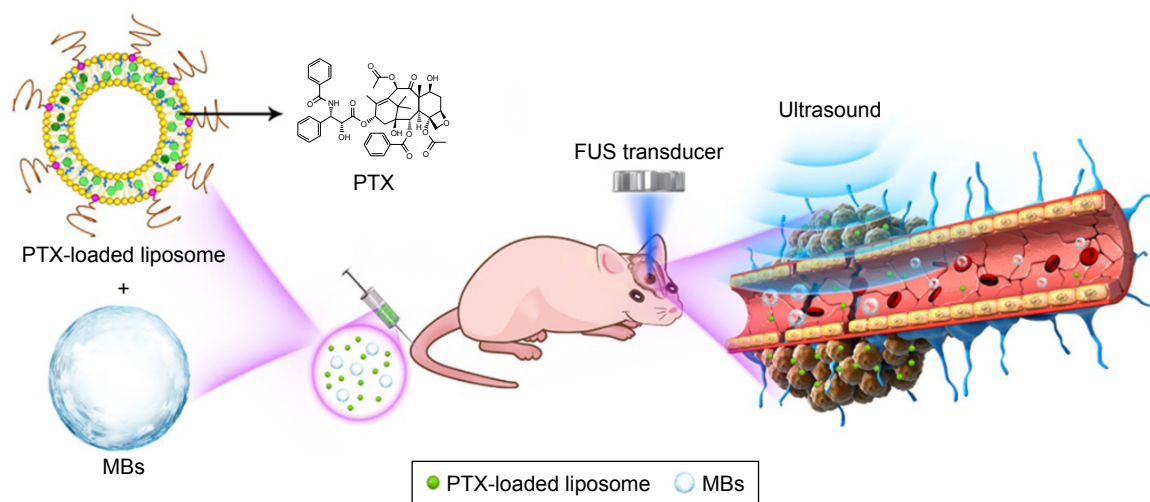

Figure 1 Schematic illustration outlining the delivery of PTX-LIPO using FUS exposure in the presence of circulating MBs.
Notes: Stabilized long-circulating liposomes loaded with paclitaxel were co-injected with MBs through the tail vein of nude mice with intracranial glioblastoma xenografts. Low-intensity pulsed FUS sonication was applied to the GBM xenograft through the intact skull. PTX was delivered into the GBM tissue through the BTB disrupted by FUS with MBs.
Abbreviations: BTB, blood–tumor barrier; FUS, focused ultrasound; GBM, glioblastoma multiforme; MBs, microbubbles; PTX, paclitaxel; PTX-LIPO, paclitaxel liposomes.

Materials and methods
Preparation of drug-loaded liposomes and MBs

In this study, stabilized long-circulating PTX-LIPO were prepared as previously described (Figure 2A).[17] Briefly, a lipid solution consisting of 1,2-dipalmitoyl-sn-glycero-3-phosphocholine (DPPC) (Lipoid, Ludwigshafen, Germany):PTX (Chengdu Yuancheng Biotechnology Ltd. Co., Chengdu, China): N-(carbonyl-methoxypolyethylene glycol-2000)-1,2-distearoyl-sn-glycero-3-phosphoethanolamine (DSPE-PEG2000) (Lipoid):cholesterol (Lipoid) at a molar ratio of 80:10:10:5 was prepared such that the final PTX concentration was 1 mg/mL. The solution was then extruded through a polycarbonate membrane with 200 nm pores. Liposomes loaded with IR-780 iodide (IR780-LIPO; Sigma-Aldrich, St Louis, MO, USA), a fluorescent probe for in vivo imaging, were also prepared using the same method in this study. The size distribution of the liposomes was measured by a Zetasizer Nano ZS90 (Malvern Instruments, Malvern, UK). The morphology of PTX-LIPO was examined using a transmission electron microscope (Tecnai G2 F20 S-TWIN; FEI Company, Hillsboro, OR, USA).

MBs with a lipid shell and a perfluoropropane (C_3F_8, 99.999% purity; Xundong Gas Technology, Suzhou, China) gas core were prepared in-house, as described in our previous study.[18] Briefly, the MBs were coated with 1,2-distearoyl-sn-glycero-3-phosphocholine (DSPC):DSPE-PEG2000 at a molar ratio of 9:1. The final lipid concentration was 3 mg/mL. The concentration and particle size distribution were measured using a Coulter Counter Multisizer IV (Beckman Coulter Inc., Miami, FL, USA) after dilution with Isoton II. The aperture diameter used in the measurement was 20 µm, with the corresponding measurement range from 0.4 to 12 µm. To investigate the lifetime of MBs in the brain, contrast-enhanced ultrasound imaging was performed on mice after craniotomy surgery using a small animal ultrasound imaging system (S-Sharp Corporation, New Taipei City, Taiwan) with a 40 MHz transducer (Figure 3A and B). Time intensity curves were acquired from a series of contrast images.

In vitro cytotoxicity of PTX-LIPO toward glioblastoma cells

In this study, human glioblastoma cell line U87 MG (ATCC, Manassas, VA, USA) was used. The cells were cultured in DMEM (Thermo Fisher Scientific, Waltham, MA, USA) mixed with 10% fetal bovine serum (GE Healthcare Life
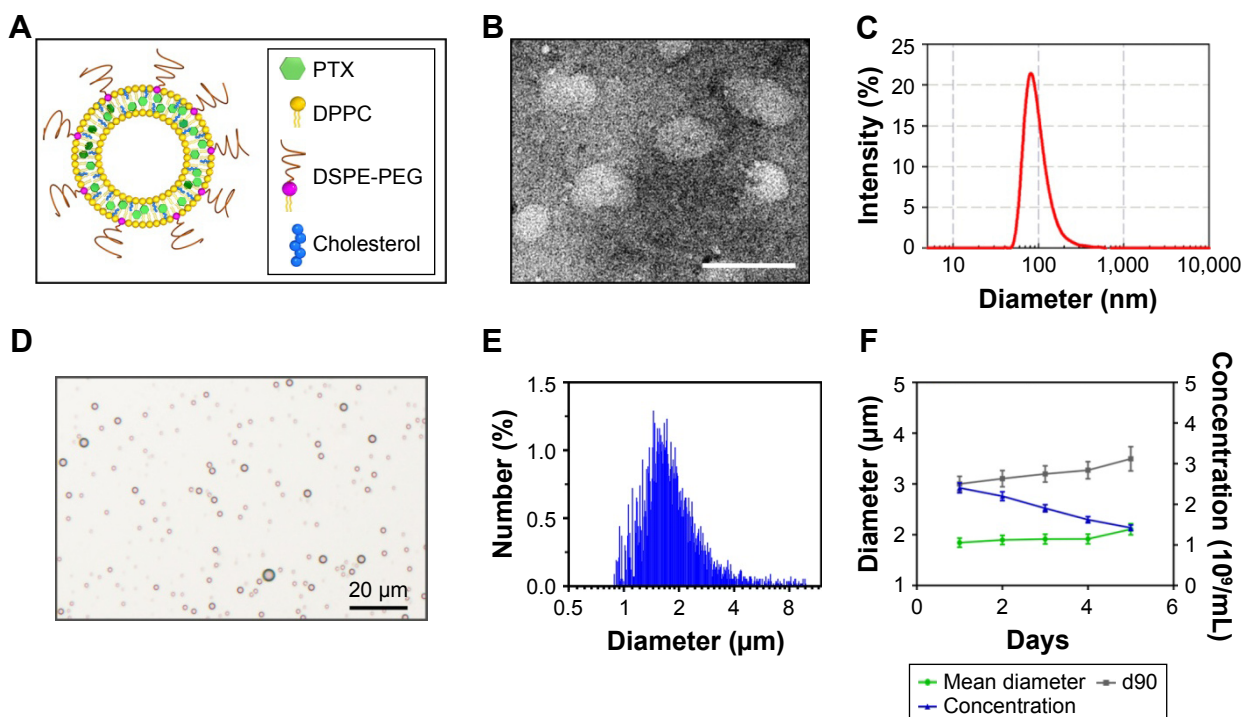

Figure 2 Characterization of the PTX-LIPO and MBs.
Notes: (**A**) Schematic of the structure of PTX-LIPO. PTX was entrapped within the liposomal phospholipid bilayer. (**B**) Transmission electron microscopy images of PTX-LIPO, bar: 100 nm. (**C**) Size distribution of PTX-LIPO. (**D**) Photomicrograph of MBs with a lipid shell and perfluoropropane core, bar: 20 µm. (**E**) Size distribution of MBs in number percent. (**F**) The variations in concentration, mean diameter and d90 of the MBs with time from the time immediately after they were freshly prepared to 5 days after preparation (n=3, mean ± SD).
Abbreviations: MBs, microbubbles; PTX, paclitaxel; PTX-LIPO, paclitaxel liposomes; d90, the size below which 90% of the particles fall.
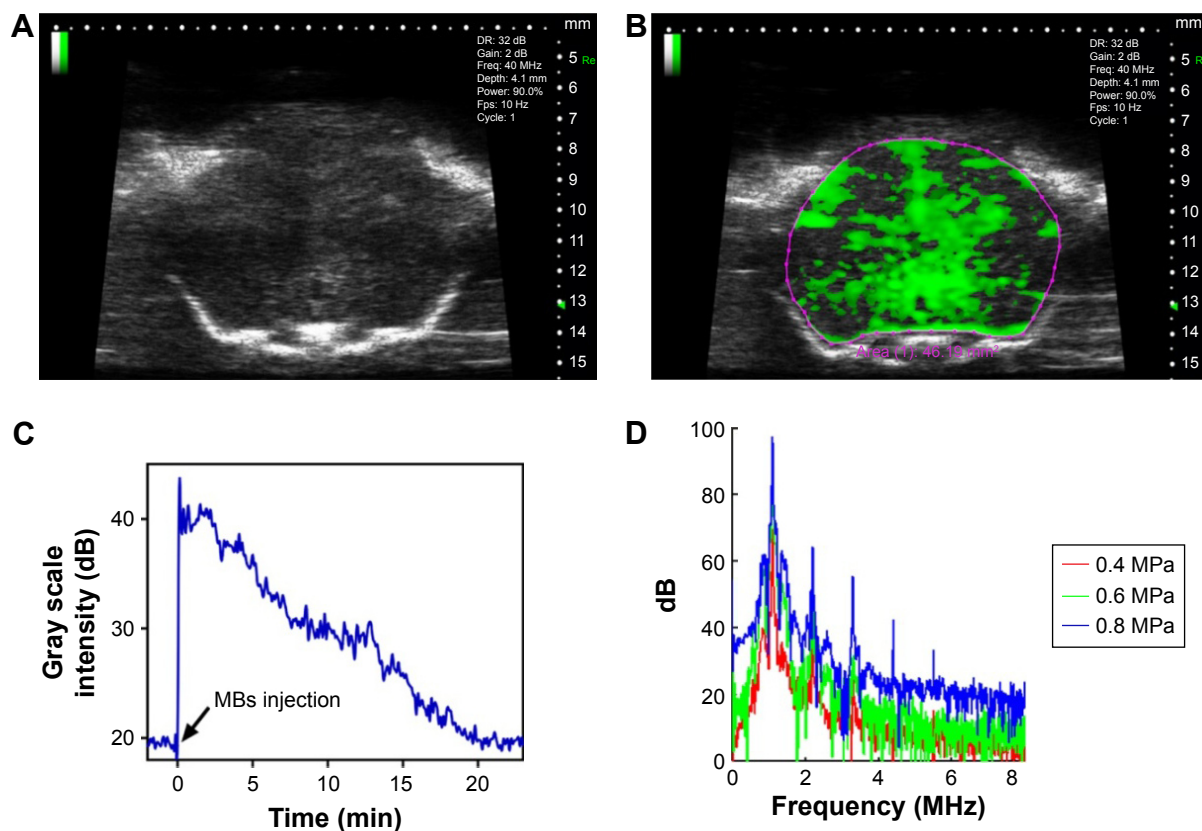
Figure 3 In vivo stability of the MBs and cavitation dose detection during the FUS-induced BBB opening.
Notes: (**A**) Contrast-enhanced B-mode images of a mouse brain before MB injection. (**B**) Contrast-enhanced B-mode images of a mouse brain after MB injection. Craniotomy surgery was performed before ultrasound imaging with a 40 MHz transducer. (**C**) Corresponding time intensity curve of contrast-enhanced B-mode images. (**D**) Spectra of the acoustic echo signals emitted by the cavitation activities of MBs during the FUS-induced BBB opening at peak-negative rarefactional pressures of 0.4, 0.6 and 0.8 MPa.
Abbreviations: BBB, blood–brain barrier; FUS, focused ultrasound; MBs, microbubbles.

Sciences, Victoria, Australia). The cells were incubated in an incubator maintained at 37°C with 5% CO_2. Cells in the logarithmic phase of growth were used.

The viabilities of U87 MG cells treated with PTX-LIPO were evaluated using a Cell Counting Kit-8 assay. Briefly, U87 MG cells (1×10^4 cells/well) were seeded into 96-well plates for 24 h and then incubated with 0, 0.01, 0.5, 5, 10, 20, 40 or 100 µg/mL PTX-LIPO for 24 h overnight at 37°C. The absorbance value was measured using a microplate reader (Synergy H4; BioTek Inc., Winooski, VT, USA) at a wavelength of 450 nm. The cell viability was expressed as a percentage of the absorbance value of untreated cells.

The apoptosis of U87 MG cells treated with PTX-LIPO was also studied. Cells (5×10^5 cells/well) were cultured in a six-well plate and treated with 2 µg/mL of free PTX dissolved in dimethyl sulfoxide, 2 and 10 µg/mL of PTX-LIPO for 24 h. The cells were harvested and resuspended in 500 µL of binding buffer and incubated with 5 µL of Annexin V-fluorescein isothiocyanate and 5 µL of propidium iodide (BD Pharmingen, San Diego, CA, USA) for 15 min at room temperature in the dark. Then, the samples were analyzed using a flow cytometer (BD Accuri C6; BD Biosciences, Franklin Lakes, NJ, USA).

Increase in the permeability of the in vitro BBB model by FUS with MBs

To evaluate the effectiveness of the delivery of agents using FUS with MBs, an in vitro study on a BBB model was performed first (Figure 4A). The mouse brain capillary endothelial cell line bEnd.3 (ATCC) was cultured in DMEM mixed with 10% fetal bovine serum, 100 U/mL penicillin and 100 µg/mL streptomycin at 37°C with 5% CO_2. The in vitro BBB model was established by seeding bEnd.3 cells onto permeable transwell inserts (1×10^5 cells/insert, 12 mm diameter, 0.4 µm pore size; Corning Incorporated, Corning, NY, USA). The tight junction protein zonula occludens-1 (ZO-1) was stained with anti-ZO-1 antibody, and the nuclei of endothelial cells were stained with 4′,6-diamidino-2-phenylindole. To evaluate the functionality of the BBB model, transendothelial electrical resistance was measured
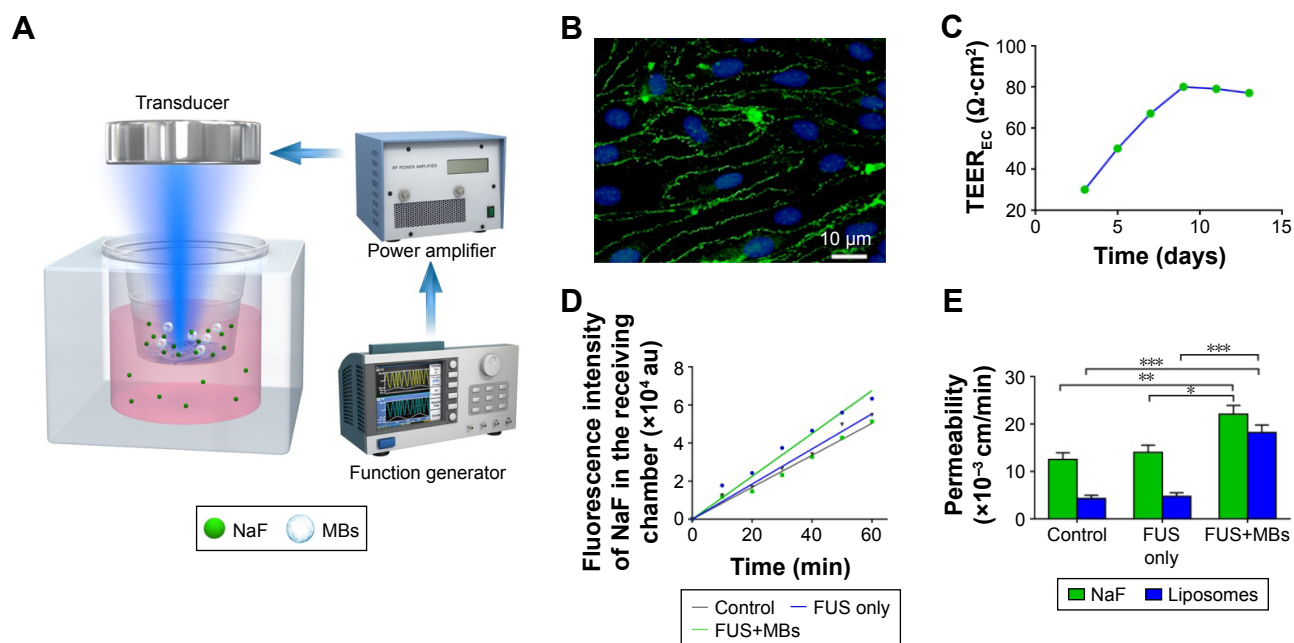
Figure 4 The effect of FUS with MBs on the permeability of the in vitro BBB model.

Notes: (**A**) Schematic of the in vitro BBB model treated with pulsed FUS exposure with MBs. (**B**) Immunofluorescence staining of tight junction protein ZO-1 (green) in the in vitro BBB model. The nuclei of bEnd.3 cells were stained with DAPI (blue). Bar: 10 μm. (**C**) TEER value variation with culture days. (**D**) The fluorescence of NaF in the receiving chamber leaking through a bEnd.3 monolayer after sonication with or without MBs. (**E**) Permeability coefficients of the bEnd.3 monolayer to NaF and rhodamine-labeled liposomes with no treatment, treatment with FUS only and treatment with FUS in the presence of MBs. Sonication was performed for 60 s with a 10 ms pulse length and 1 Hz PRF at 0.64 MPa peak-rarefactional pressure (n=3, mean ± SD). *$P < 0.05$, **$P < 0.01$, and ***$P < 0.001$.

Abbreviations: BBB, blood–brain barrier; DAPI, 4′,6-diamidino-2-phenylindole; FUS, focused ultrasound; MBs, microbubbles; NaF, sodium fluorescein; PRF, pulse repetition frequency; TEER, transendothelial electrical resistance.

using an epithelial volt-ohm meter (Millicell ERS-2; EMD Millipore, Billerica, MA, USA).

FUS was generated using a lab-made single-element spherical transducer (center frequency: 1.1 MHz, the lateral and axial full-width at half-maximum intensity of the beam: 5.0 and 65.0 mm, respectively) immersed within a cone filled with degassed water (Figure 4A). The cone tip was sealed with a thin polyurethane membrane. A function generator (AFG3102C; Tektronix, Inc., Beaverton, OR, USA) operated in burst mode was used to produce excitation signal and connected with a 50 dB power amplifier (325LA; Electronics & Innovation, Rochester, NY, USA) to drive the FUS transducer. After the cells reached confluence, MBs (5 μL/well) were diluted in culture medium and then subjected to sonication for 60 s with a 10 ms pulse length and 1 Hz pulse repetition frequency (PRF) at 0.60 MPa peak-rarefactional pressure.

To evaluate the effect of FUS with MBs on delivery of substances across the in vitro BBB model, the permeability of the bEnd.3 monolayer to sodium fluorescein (NaF, 376 Da molecular weight; Sigma-Aldrich) or rhodamine-labeled liposomes (mean diameter: 120 nm) was measured. Liposomes were prepared as described in our previous study.[18]

Briefly, 0.5 mL NaF solution (10 μg/mL) or liposomal solution (1 mg/mL) was added into the donor chamber of the insert. Next, 50 μL samples were drawn every 10 min from the receiving chamber for 60 min, and the fluorescence intensities of these successive samples were determined using a microplate reader. The total permeability was calculated as follows:[19]

$$P \text{ (in cm/min)} = (\Delta C_R / \Delta t) \times V_R / (C_D \times S),$$

where ΔC_R is the concentration increment of substances in the receiving chamber during the time interval Δt, C_D is the initial concentration in the donor chamber, V_R is the medium volume of the receiving chamber and S is the membrane surface area of the insert. The permeability of the monolayer P_M was calculated after removing the effect of the insert (P_I):

$$1/P = 1/P_M + 1/P_I$$

Intracranial glioblastoma xenograft model preparation

To evaluate therapeutic efficacy in vivo, nude mice bearing intracranial glioblastoma were prepared in this study. Male

BALB/c nude mice (6–7 weeks old, 20±2 g; the Animal Center of Southern Medical University, Guangzhou, China) were used in this study. The animals were maintained under specific pathogen-free conditions (relatively constant temperature of 24°C–26°C and humidity of 30%–50%). All animal care and experiments were performed according to a standard animal care protocol approved by the Animal Care and Use Committee of Health Science Center in Shenzhen University, China (Approval No 201505003).

All surgical instruments and supplies were sterilized before use. Mice were anesthetized with 1.5% isoflurane (RWD Life Science, Shenzhen, China), immobilized in a small animal stereotaxic apparatus (RWD Life Science) and placed on a heating pad at 37°C±1°C to maintain their body temperature. A skin incision was made on the top of the skull after antisepsis and a burr hole was drilled into the skull of the right hemisphere. Then, 1×10^5 U87 MG cells suspended in 2 µL of PBS were injected into the right striatum through the hole using a 26s-gauge needle (Hamilton, Reno, NV, USA) driven by a microsyringe pump (UMP3 controlled by SYS-Micro 4; World Precision Instruments, Sarasota, FL, USA) at a speed of 400 nL/min. Magnetic resonance imaging (MRI) was performed on the 10th day after surgery to determine whether the glioblastoma xenograft was implanted successfully.

Experimental design of the in vivo therapeutic study

The in vivo animal study was then performed to evaluate therapeutic efficacy. A total of 82 nude mice bearing U87 MG glioblastoma were used in this study. They were divided into four experimental groups.

In experimental group 1, 12 nude mice bearing orthotopic glioblastoma were used to validate the effectiveness of drug delivery using FUS with MBs. First, six nude mice treated with FUS in conjunction with MBs and Evans blue dye (EB, 1%) were used to verify the increase in the BTB permeability resulting from this treatment method. Meanwhile, the cavitation signals during FUS sonication were detected and analyzed. To compare the difference between the accumulation of liposomes that penetrate through BTB compromised by glioma and those that penetrate through BTB disrupted by FUS, another six nude mice in this group were injected in the bilateral striatum with the same amount of U87 MG cells. FUS was applied to the right glioblastoma after IR780-LIPO along with MBs were injected, while the left tumor was unsonicated. Cardiac perfusions were performed, and the brains were extracted from the skull 4 h

later. Then, the extravasation of IR780-LIPO was detected using an in vivo imaging system (IVIS II; PerkinElmer Inc., Waltham, MA, USA).

In experimental group 2, 18 nude mice were used to assess the pharmacokinetics and biodistribution of PTX. The mice were randomly divided into two subgroups: one treated with only PTX-LIPO injections (n=9) at a dose of 10 mg/kg body weight and the other treated with PTX-LIPO (at a dose of 10 mg/kg) delivered via FUS with MBs (FUS+MB+PTX-LIPO: n=9) at 2 weeks postimplantation. Tissue samples were collected at three time points: 1, 2 and 3 h after the treatment (n=3 at each time point).

Afterward, experiments were performed to investigate the therapeutic outcomes through longitudinal intracranial tumor growth monitoring by MRI on glioma-bearing nude mice after a 1-week session of treatment as well as the survival time of these animals. Forty nude mice were randomly divided into four subgroups in experimental group 3: the untreated control subgroup (Control: n=10), the group treated with only FUS with MBs (FUS+MB: n=10), the group treated with only PTX-LIPO injections (n=10) and the group treated with PTX-LIPO delivered via FUS with MBs (FUS+MB+PTX-LIPO: n=10). A total of three times of treatments were administered every other 2 days over 1 week. This session was started 10 days after the tumor cell implantation. The intracranial tumor growth of nude mice in each subgroup was monitored by MRI. The survival time of each nude mouse was also recorded.

In experimental group 4, immunohistochemical analysis was performed on the nude mice to assess tumor proliferation and apoptosis. Three glioma-bearing nude mice were untreated and used as a control. Nine animals were treated with FUS+MB, PTX-LIPO or FUS+MB+PTX-LIPO (each treatment: n=3). Two days after treatment, cardiac perfusions were performed. The brains were extracted from the skull and postfixed in 4% paraformaldehyde for at least 24 h.

In vivo sonication procedures

A tumor-bearing mouse was anesthetized with 1.5% isoflurane and the head was immobilized with ear bars. It was placed in the prone position on a heating pad at 37°C±1°C to maintain the body temperature. The same FUS transducer from the in vitro study was used, with the tip located above the mouse's head, coupled with ultrasound gel medium in order to transmit the ultrasonic beam into the tumor with minimal attenuation. The transducer was driven by the same sonication apparatus that was used in the in vitro study. The sonication procedure was as follows: MBs (0.2 µL/g of body

weight) were co-injected with PTX-LIPO (10 mg/kg of body weight) through the tail vein twice; each time, 0.1 mL of the solution was injected with a 3 min interval between the two. Sonication was started ~15 s after the injection (pulse length: 10 ms, PRF: 1 Hz, time: 60 s). It was found in our previous study that 120 nm liposomes accumulated in the brain more at 0.64 MPa, while the delivery outcome was very limited at 0.53 MPa; therefore, the peak-rarefactional pressure used in this study was 0.64 MPa.[18] The left hemisphere was not sonicated. The peak-rarefactional pressure amplitude presented in this study was not corrected due to skull attenuation effects.

The physiologic changes in the BBB have been considered to be closely associated with the mechanical effects of the cavitation activity of MBs in an ultrasonic field.[20–22] In this study, the acoustic emissions emitted by oscillating MBs during FUS-induced BBB opening were recorded using a highly sensitive and broad-bandwidth hydrophone (frequency range: 10 kHz–15 MHz; Sonic Concepts, Bothell, WA, USA), which was confocally and coaxially aligned with an FUS transducer (1.1 MHz, Sonic Concepts). Prior to the MB administration, a 2 s sonication was applied in order to obtain the baseline acoustic response. Echo signals received by the hydrophone were amplified by a pulser-receiver system (model 5900PR; Panametrics, Kennewick, WA, USA) and sampled at a 100 MHz sampling rate using a high-speed digitizer (model PCIe-9852; ADLink Technology Inc., New Taipei City, Taiwan). Spectral analysis of the signals was subsequently conducted.

Biodistribution of PTX

The biodistribution of PTX was assessed 1, 2 and 3 h after only PTX-LIPO or FUS+MB+PTX-LIPO treatment on nude mice with implanted U87 MG cells. Blood samples and organs, including the glioma, heart, liver, spleen, lungs, kidneys and brain, were harvested. The blood samples were further processed into plasma. The organ samples were weighed and frozen at −80°C before further processing. When all samples were prepared, the tissues were homogenized using a homogenizer (Bio-Gen Series PRO200; PRO Scientific, Oxford, CT, USA). PTX was extracted with 1 mL of methanol, and the samples were centrifuged at 12,000 rpm for 15 min. The clear supernatants were collected and dried under a nitrogen flow. Then, the residue of each sample was dissolved in 300 µL methanol (Sinopharm Chemical Reagent Co., Ltd., Shanghai, China) and filtered through a 0.22 µm polyamide nylon filter (JinTeng, Tianjin, China). The filtrate was used as the sample solution. The

concentration of PTX was analyzed using high-performance liquid chromatography.

MRI and survival data analysis

The progression of the intracranial U87 MG glioblastoma was longitudinally monitored by a 3 T MRI system (TRIO 3-T MRI; Siemens MEGNETOM, Munich, Germany) every week from day 10 up to day 38 after the tumor cell implantation. The anesthetized mice were placed in a plexiglass holder in the center of the magnet. A 5.0 cm diameter transmit/receive surface coil for small animals was used. T2-weighted images of the brain were acquired (repetition time/echo time: 2030/75 ms; matrix: 256×256; field of view: 32×32 mm^2; slice thickness: 1.0 mm) in coronal and horizontal planes. The tumor volumes were calculated based on the modified ellipsoidal formula:[23]

$$\text{Tumor volume (in mm}^3\text{)} = (\text{length} \times \text{width}^2) \times 0.5.$$

The survival time of the nude mice after different treatments was recorded from the day of the tumor implantation until death. Survival curves of the four subgroups in experimental group 3 were plotted using the Kaplan–Meier method, and the statistical significances were analyzed by the Mantel–Cox log-rank test. The medium and mean survival time, increase in median and mean survival time (IST$_{median}$ and IST$_{mean}$) and maximal survival time were compared. A P-value of <0.05 was considered to be significant.

Immunohistochemical analysis

In experimental group 4, 12 mice were randomly divided into four subgroups: the control group and the mice treated with FUS+MB, PTX-LIPO or FUS+MB+PTX-LIPO. Two days after treatment, the implanted glioma tissue was extracted and postfixed for at least 24 h. They were then embedded in paraffin and sliced into 5 µm sections.

To evaluate tumor cell proliferation, sections were stained with Ki-67 and proliferating cell nuclear antigen (PCNA) antibodies. Briefly, dewaxed sections were incubated with 3% H$_2$O$_2$ solution and the primary anti-Ki-67 antibody (1:50 dilution; Abcam, Cambridge, MA, USA) or anti-PCNA antibody (1:50 dilution, Abcam) at 4°C overnight. To assess tumor cell apoptosis, sections were stained using the terminal deoxynucleotidyl transferase-mediated dUTP nick end labeling (TUNEL) assay (Jiancheng Bioengineering Institute, Nanjing, China). Positive and negative immunohistochemical controls were performed.

Slices were imaged using a microscope (BX53; Olympus Corporation, Tokyo, Japan) and immunohistochemical evaluations were quantified using cellSens Dimension software (Olympus Corporation). The positive index was defined as the percentage of positive cells out of at least 2,000 tumor cells at 200× magnification.

Statistical analysis

All data were expressed as the mean ± SD. The statistical analysis of the data, including the in vitro and in vivo data, was carried out using one-way analysis of variance. The significance was analyzed by using the Tukey–Kramer test method. Differences were considered significant when *$P<0.05$, **$P<0.01$ and ***$P<0.001$, respectively.

Results

Characterization of PTX-LIPO and MBs

In this study, PTX was entrapped within the liposomal phospholipid bilayer as illustrated in Figure 2A. Transmission electron microscopy images showed that the PTX-LIPO exhibited a spherical shape (Figure 2B). The mean diameter of the liposomes was 98.3 nm, and the polydispersity index was 0.171 (Figure 2C), implying uniform distribution.

MBs were polydispersed with sphere shapes (Figure 2D and E) with the number-weighted mean diameter of the freshly prepared MBs being 1.932 μm, a value that increased slightly over time. At day 5 after preparation, it had become 2.100 μm, representing an increase of 8.7% (Figure 2F). D90, representing the size below which 90% particles fall, was 2.980 μm after fresh preparation and increased by 17.4% to 3.500 μm 5 days later (Figure 2F). The concentration of the freshly prepared MBs was 2.5×10^9/mL, and it gradually decreased to 1.2×10^9/mL after 5 days (Figure 2F). These results indicated that the prepared MBs were relatively stable.

In vivo stability of MBs and cavitation dose detection

The in vivo stability of the MBs was evaluated through contrast-enhanced imaging of brain tissue with a 40 MHz transducer over 20 min. As shown in Figure 3A and B, the brain image contrast was significantly enhanced after the injection of MBs into the tail vein. The corresponding signal intensity increased up to 40 dB and dropped down to the initial amplitude level ~20 min after administration (Figure 3C).

The cavitation effects of the prepared MBs during the in vivo BBB opening were investigated. Stable cavitation

is manifested by harmonic and sub/ultraharmonic acoustic emissions in the frequency domain, while inertial cavitation is indicated by a broadband signal.[24] As shown in Figure 3D, at 0.6 MPa, a slightly higher harmonic and ultraharmonic signal was observed compared to the case at 0.4 MPa, indicating a stronger stable cavitation effect. However, at an acoustic pressure of 0.8 MPa, a pronounced broadband signal appeared, indicating that the inertial cavitation effect was augmented. Therefore, the acoustic pressure of 0.64 MPa, which was lower than 0.8 MPa, was used in the in vivo study.

The effect of FUS exposure in the presence of MBs on permeability of the in vitro BBB model

In this study, monolayers of bEnd.3 cells were cultured to mimic the BBB in vitro. Approximately 7 days after seeding, bEnd.3 cells on the membranes of inserts reached confluence. Tight junction protein ZO-1, which is located between the membranes of adjacent endothelial cells, could be observed through immunofluorescence staining (Figure 4B). The transendothelial electrical resistance value was observed to steadily increase over time and reached 80 $\Omega\cdot cm^2$ on the ninth day after seeding (Figure 4C). The fluorescence intensity of NaF leaking through the bEnd.3 monolayer into the receiving chamber increased linearly with time (Figure 4D). The in vitro BBB permeability to NaF was 0.013±0.001 cm/min (Figure 4E). These results suggested that the monolayer of bEnd.3 cells had a paracellular barrier property.

After reaching confluence, the in vitro BBB model was used to evaluate the effect of FUS in the presence of MBs on permeability. In the absence of MBs, the permeability of the bEnd.3 monolayer treated by FUS to NaF or liposomes was similar with that of the control. However, in the presence of MBs, FUS induced a significantly increased permeability to NaF: 0.022±0.002 cm/min, or 77% larger than the control, as well as an increased permeability to liposomes, by 4.25-fold of the control.

In vitro antiglioma effect of PTX-LIPO

The in vitro antiglioma effect of the prepared PTX-LIPO was evaluated. As shown in Figure 5A, the viability of U87 MG cells decreased from 82.4% to 48.7% when the concentration of PTX increased from 0.01 to 100 μg/mL. This result showed an in vitro antiproliferation effect of PTX-LIPO on U87 MG cells. As shown in Figure 5B–F, apoptosis and necrosis ratio of cells treated by 2 and 10 μg/mL PTX-LIPO increased to by 18.0% and 23.1%, respectively. The result
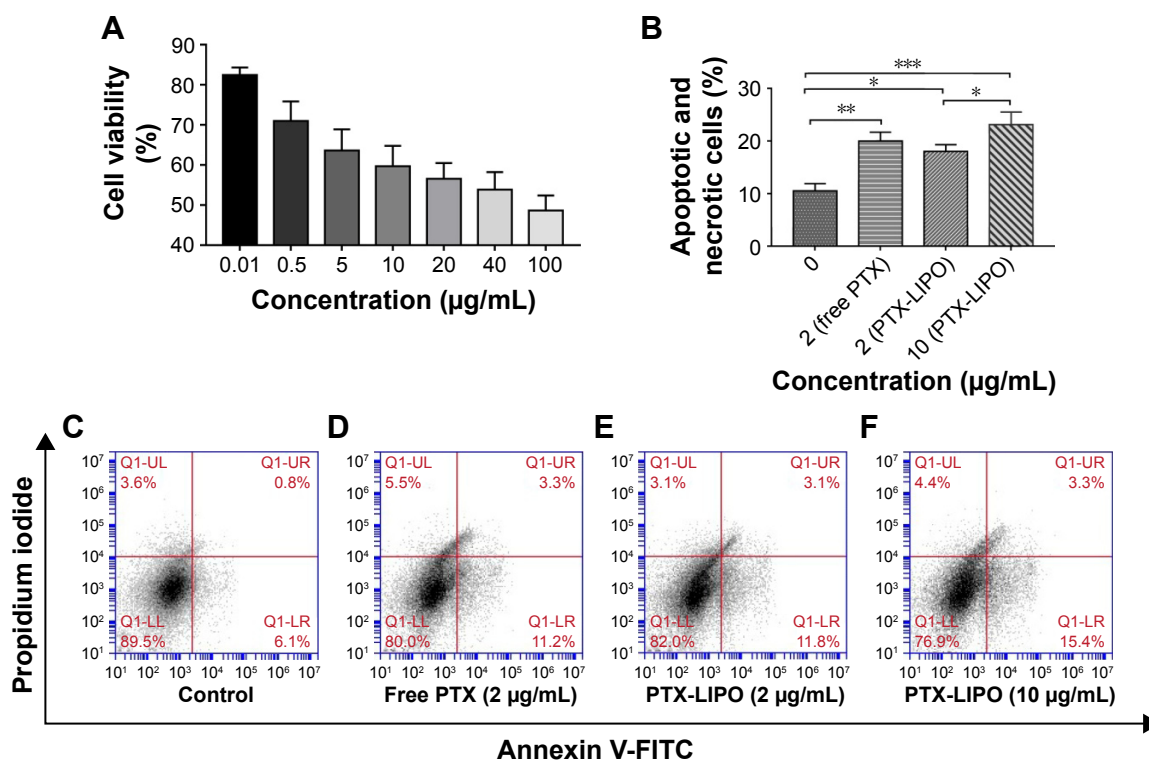
Figure 5 In vitro antiglioma effect of PTX-LIPO.
Notes: (**A**) The viability over 24 h of U87 MG cells treated with PTX-LIPO at concentrations ranging from 0.01 to 100 µg/mL (n=3, mean ± SD). (**B**) The percentages of apoptotic and necrotic cells determined by the apoptosis study of U87 MG cells in the following: control group (**C**), group treated with 2 µg/mL free PTX (**D**) and groups treated with PTX-LIPO at concentrations of 2 µg/mL (**E**) and 10 µg/mL (**F**) (n=3, mean ± SD). *$P<0.05$, **$P<0.01$, and ***$P<0.001$.
Abbreviations: FITC, fluorescein isothiocyanate; PTX-LIPO, paclitaxel liposomes.

confirmed that the prepared PTX-LIPO could induce a significant in vitro antiglioma effect on U87 MG cells.

Comparison between substances penetrating incomplete glioma BTB and those penetrating FUS-triggered disrupted BTB

It is well known that the BTB is compromised in the glioma vasculature, giving it leaky properties and making it easier for molecules to pass through it.[25] A study on the comparison between accumulated substances penetrating through the leaky glioma microvasculature and those penetrating through the FUS-induced disrupted BTB was then performed (Figure 6A). As shown in Figure 6B, enhanced EB extravasation was observed to be induced by FUS exposure with MBs, compared to slight EB extravasation from the leaky glioma vasculature itself. Note that without treatment with FUS and MBs, EB was distributed heterogeneously within the tumor region. However, after insonification in the presence of MBs, EB spread throughout most of the tumor region.

The enhanced effect on delivery of liposomes by using FUS with MBs was investigated through the examination of

the penetration of fluorescence dye (IR780)-loaded liposomes through the BTB. FUS was only introduced to the intracranial glioblastoma growing in the striatum of the right hemisphere of the nude mice. As shown in Figure 6C, liposome extravasation was observed in bilateral tumors. Moreover, it was noticed that the accumulation of liposomes in the right glioblastoma was enhanced, compared to that in the left tumor. The quantification of fluorescence signals showed a level of liposome deposition in the right tumor region 3.14-fold greater than that in the left tumor site (Figure 6D). The results confirmed that FUS with MBs effectively enhanced liposome delivery after BTB disruption.

Biodistribution of PTX-LIPO

The drug concentration in the organs and plasma after treatment was quantified using high-performance liquid chromatography. It was found that PTX accumulated in the liver the most and then the lungs, indicating nonspecific uptake in these organs 1 h after treatment (Figure 7A). There was no significant difference in PTX distribution in the heart and spleen between the two groups. However, for nude mice treated with FUS+MB+PTX-LIPO, the amount of
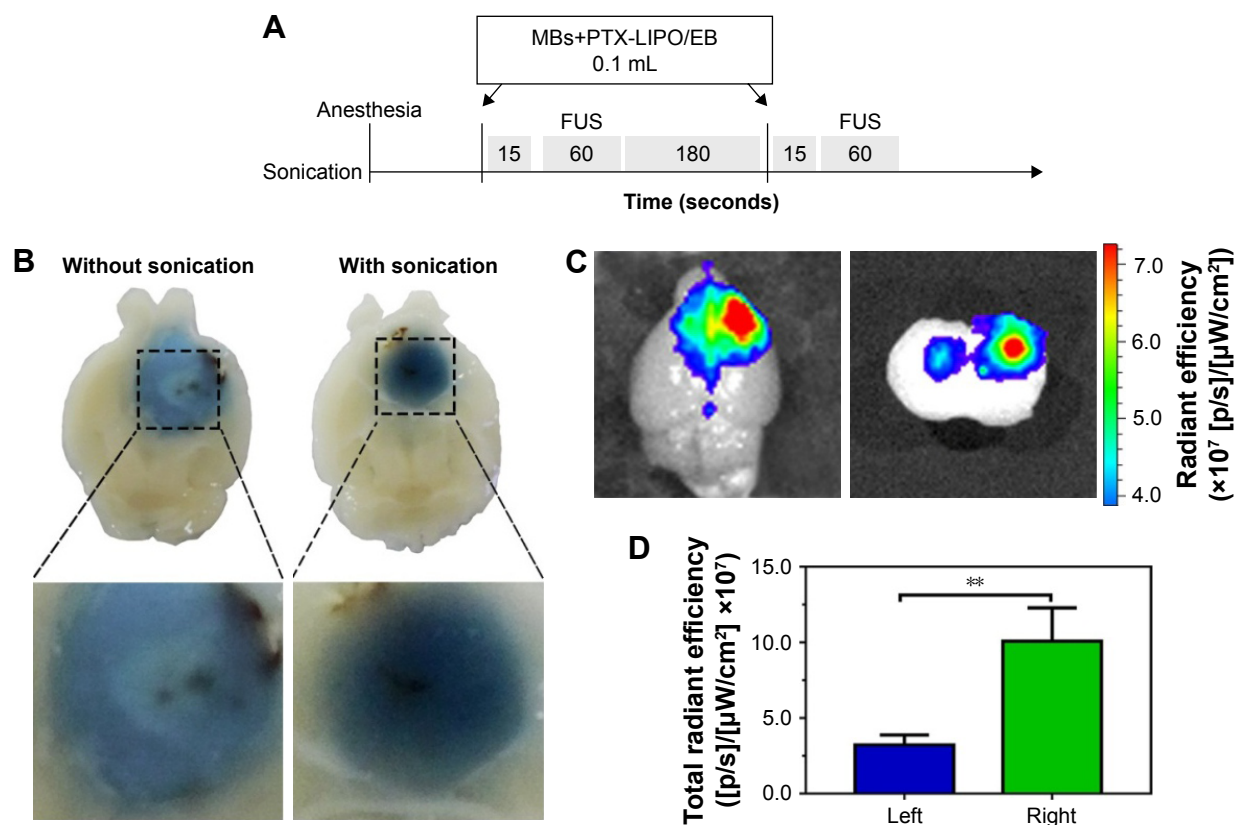
Figure 6 Comparisons of the EB dye or liposomes that penetrate through BTB-compromised glioma to those that penetrate through the BTB disrupted by FUS.
Notes: (**A**) Experimental timeline of the treatment procedure of the BTB opening in vivo induced by FUS with MBs. (**B**) EB extravasation in glioblastoma. Left: without FUS sonication with MBs. Right: with FUS sonication with MBs. Note that without treatment with FUS or MBs, EB was distributed heterogeneously within the tumor region. However, after insonification in the presence of MBs, EB spread throughout most of the tumor region. (**C**) Liposome accumulation in tumor regions through the glioma-compromised BTB (left) and FUS-disrupted BTB (right). The same amount of U87 MG cells was implanted in the bilateral striatum in the nude mouse brains. FUS was only introduced to the right intracranial glioblastoma. (**D**) Fluorescence intensity of the extravasated liposomes in the left and right tumor regions (n=6, mean ± SD). **$P<0.01$.
Abbreviations: BTB, blood–tumor barrier; EB, Evans blue; FUS, focused ultrasound; MBs, microbubbles; PTX-LIPO, paclitaxel liposomes.

PTX accumulated in liver and kidneys decreased by 12.81% (P=0.031) and 27.89% (P=0.017), respectively, along with a 9.44% increase in the amount of PTX in the lung (P=0.33). In addition, FUS with MBs induced more PTX deposition in glioma 1 h after treatment, achieving 1.85±0.58 µg/g tissue, which was 3-fold greater than in the case of mice treated only with PTX-LIPO injection (P=0.02).

The concentrations of PTX in the plasma and glioma of nude mice in two subgroups were also investigated up to 3 h after receiving PTX-LIPO only or FUS+MB+PTX-LIPO treatment. As shown in Figure 7B, PTX concentration decreased along with the circulation time and there was only slight difference between the two subgroups at 1 h after treatments. Although the drug deposition in the glioma of nude mice subjected to PTX-LIPO only treatment increased with time due to the enhanced permeability and retention effect of GBM, the amount of PTX delivered using FUS combined with MBs was significantly enhanced, reaching

7.20±1.18 µg/g in glioma, which was 2-fold greater than the PTX-LIPO only group 3 h after treatment (Figure 7C).

In vivo therapeutic efficacy of PTX-LIPO delivered by FUS with MBs

The growth of intracranial glioblastoma xenografts was longitudinally monitored using T2-weighted MRI every week before and after treatments (Figure 8A). As shown in Figure 8B and C, the tumors in the untreated control mice brains exhibited an exponential growth pattern: from 0.50±0.10 mm³ on day 10 to 7.36±6.14 mm³ on day 24 and then dramatically increasing to 94.61±27.45 mm³ on day 38 after implantation. For mice treated with FUS+MBs without the delivery of PTX-LIPO, their tumors grew rapidly with a similar tendency as the control group, reaching 93.31±31.12 mm³ on day 38. The growth of glioma in nude mice treated with PTX-LIPO only seemed to be delayed until 2 weeks after treatment, when the tumors continued to grow
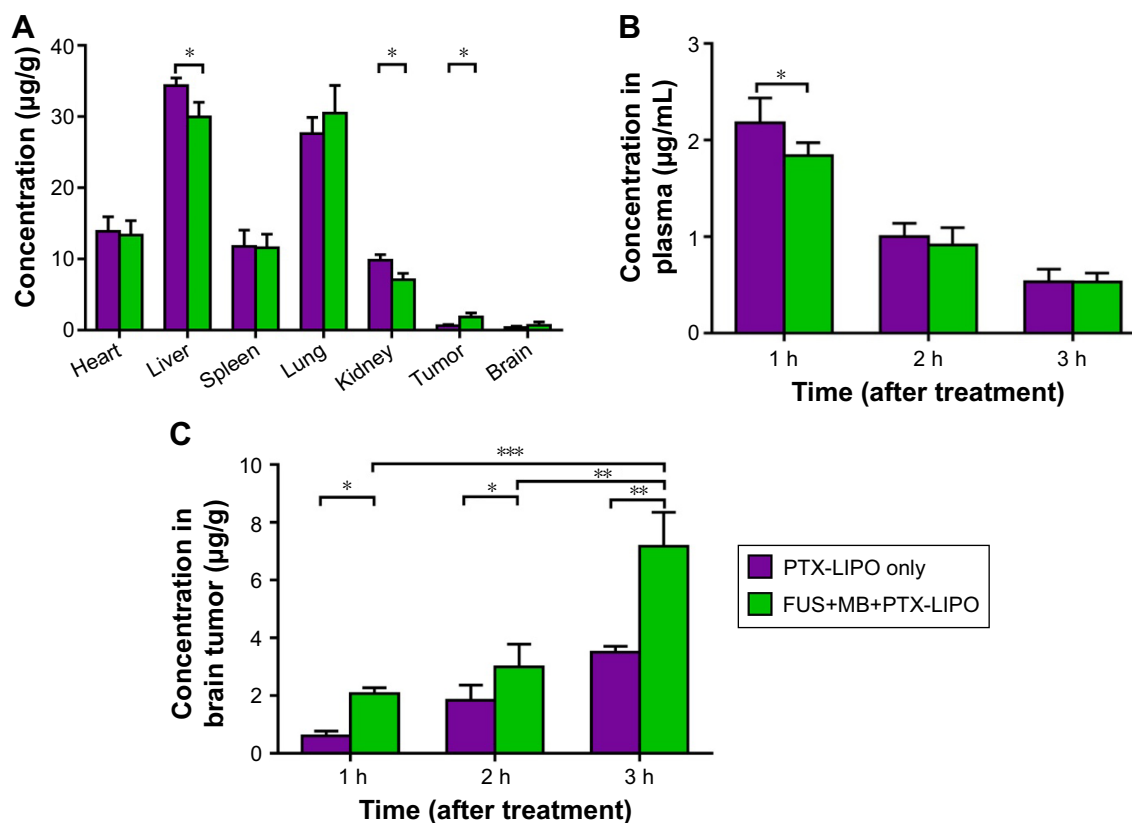
Figure 7 The biodistribution of PTX in nude mice receiving PTX-LIPO only or FUS+MB+PTX-LIPO treatment.
Notes: The drug concentration in the organs and plasma after treatment was quantified using HPLC (n=3, mean ± SD). (**A**) PTX concentration accumulated in the glioma, heart, liver, spleen, lungs and kidneys of nude mice 1 h after they received PTX-LIPO or FUS+MB+PTX-LIPO treatment. PTX concentrations in (**B**) plasma and (**C**) brain tumors at 1, 2 and 3 h after the PTX-LIPO or FUS+MB+PTX-LIPO treatment. *$P<0.05$, **$P<0.01$, and ***$P<0.001$.
Abbreviations: PTX, paclitaxel; PTX-LIPO, paclitaxel liposomes; MBs, microbubbles.

rapidly, reaching 35.59±8.13 mm^3 on day 38. Distinctively, in the subgroup of nude mice treated with FUS+MB-enhanced PTX-LIPO chemotherapy, tumor growth was suppressed consistently throughout the 4 weeks following the treatment. The tumor volume increased much slower than that of the control group: from 0.48±0.06 mm^3 on day 10 to 0.40±0.37 mm^3 on day 24 and finally to 0.87±0.76 mm^3 on day 38 after implantation. This result suggested that enhanced PTX-LIPO delivery facilitated by FUS with MBs improved the inhibitory effect of the formulation on glioma progression.

To further evaluate the therapeutic efficacy of enhanced PTX-LIPO delivery using FUS with MBs, the survival times of four subgroups of nude mice that received different treatments (Control, FUS+MB, PTX-LIPO and FUS+MB+PTX-LIPO) were recorded. The Kaplan–Meier survival curves of the four subgroups were plotted, as shown in Figure 8D, and the corresponding statistical data are summarized in Table 1. The median survival time of the untreated control group and the FUS+MB group was 31.5 and 30.5 days, respectively, without any significant difference. Although the mice treated with PTX-LIPO only had a 5.2% greater median survival time

than the untreated mice, this difference was not statistically significant ($P=0.0744$). In contrast, the enhanced delivery of PTX-LIPO via FUS with MBs prolonged the median survival time to 46.5 days, resulting in a statistically significant ($P=0.0003$) increase of 20.8% compared to that of the control group. Equivalent results were also observed in terms of the mean survival times of the four subgroups. Moreover, the maximal survival day in the FUS+MB+PTX-LIPO group was 58 days, an increase of 34.9% compared to that in the control group. These in vivo experimental results further demonstrated that the therapeutic efficacy of nude mice bearing intracranial U87 MG glioblastoma was effectively improved by treatment with enhanced PTX-LIPO delivered via FUS with MBs.

Immunohistochemical analysis

To further evaluate the therapeutic effects on tumor cell proliferation in different treatment groups, immunohistochemical staining with PCNA and Ki-67 antibodies was performed in this study. As shown in Figure 9A–C, abundant PCNA-positive and Ki-67-positive cells were observed in
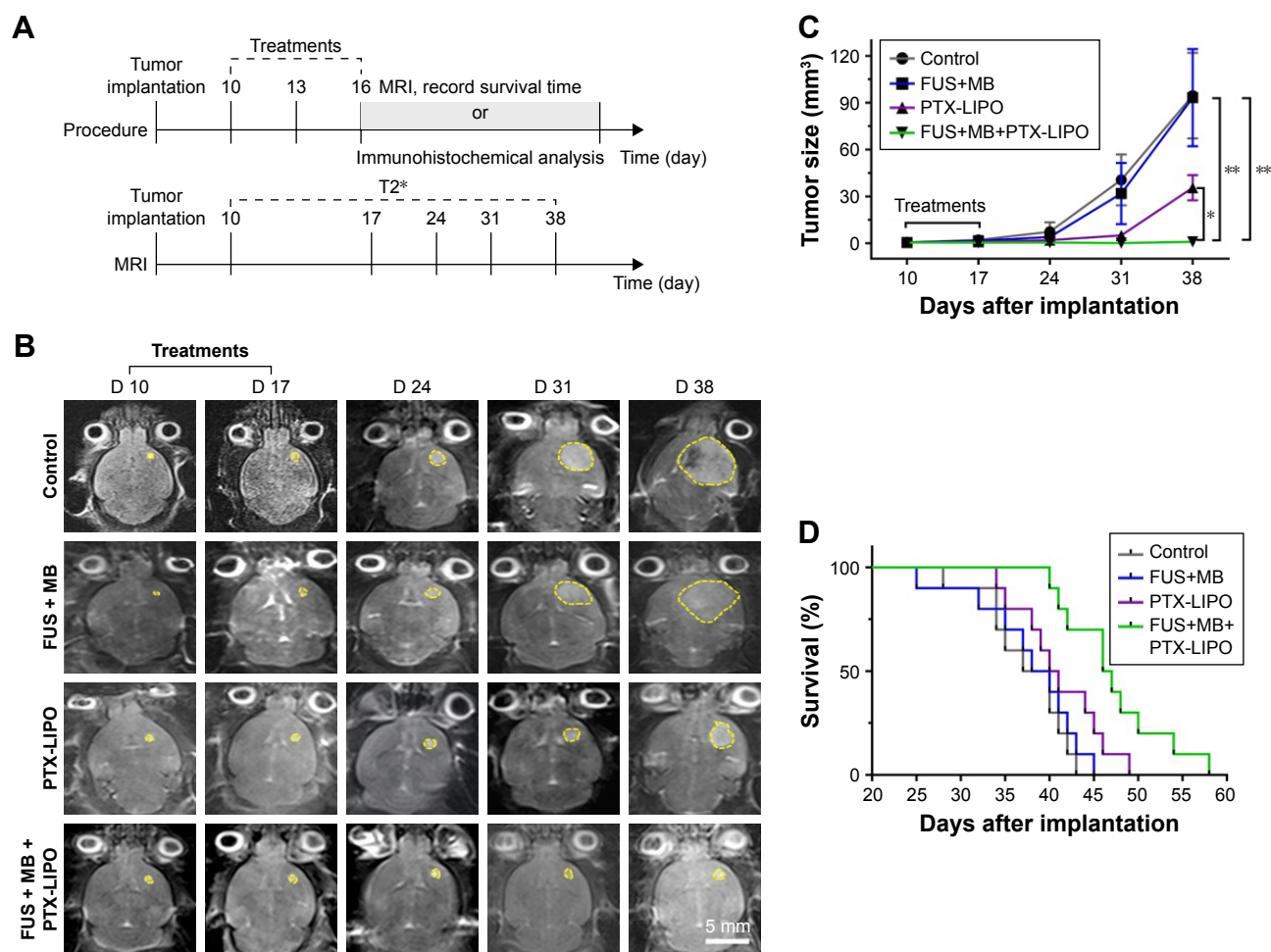
Figure 8 In vivo antiglioma efficacy in nude mice bearing intracranial glioblastoma in different treatment groups: no treatment as the Control, FUS exposure with MBs but without PTX-LIPO as FUS+MB, PTX-LIPO injection only and PTX-LIPO delivery using FUS with MBs as FUS+MB+PTX-LIPO.
Notes: (**A**) Experimental timeline of the treatment procedure and MRI longitudinal study. Treatments were started from the 10th day after the glioma cell implantation every other 2 days for a total of three times. (**B**) Representative T2-weighted MRI horizontal images of intracranial U87 MG glioblastoma progression (yellow outline) before and after different treatments. Bar: 5 mm. (**C**) Tumor volumes from day 10 to day 38 after implantation of nude mice with different treatments (n=10, mean ± SD). *$P<0.05$ and **$P<0.01$. (**D**) The Kaplan–Meier survival curves of nude mice in each treatment group.
Abbreviations: FUS, focused ultrasound; MBs, microbubbles; MRI, magnetic resonance imaging; PTX-LIPO, paclitaxel liposomes.

untreated glioma regions, accounting for 66.4% and 66.1% of all cells, respectively. There were no significant differences in tumor cell proliferation in the FUS+MB group and the PTX-LIPO group, as indicated by the microscopy examination and quantitative analysis. However, the number of PCNA-positive and Ki-67-positive cells dramatically decreased in tumors subjected to PTX-LIPO chemotherapy enhanced by FUS with MBs, representing 17.8% and 24.8% of all cells, respectively (Figure 9B and C). These results indicated that glioma proliferation was evidently inhibited by the enhanced delivery of PTX-LIPO via the approach of using FUS with MBs.

Table 1 Survival analysis of the nude mice in the four treatment groups

Groups	Median survival days	IST$_{median}$ (%)	Mean survival days	IST$_{mean}$ (%)	Maximal survival days	P-value
Control (n=10)	38.5		37.4±4.7		43	
FUS+MB (n=10)	39	1.3	37.8±5.9	1.1	45	0.5198
PTX-LIPO (n=10)	40.5	5.2	41.1±4.9	9.9	49	0.0744
FUS+MB+PTX-LIPO (n=10)	46.5	20.8	47.2±5.7	26.2	58	0.0003

Note: Data presented as mean ± standard deviation.
Abbreviations: FUS, focused ultrasound; IST$_{median}$, increase in the median survival time; IST$_{mean}$, increase in the mean survival time; MB, microbubble; PTX-LIPO, paclitaxel liposomes.
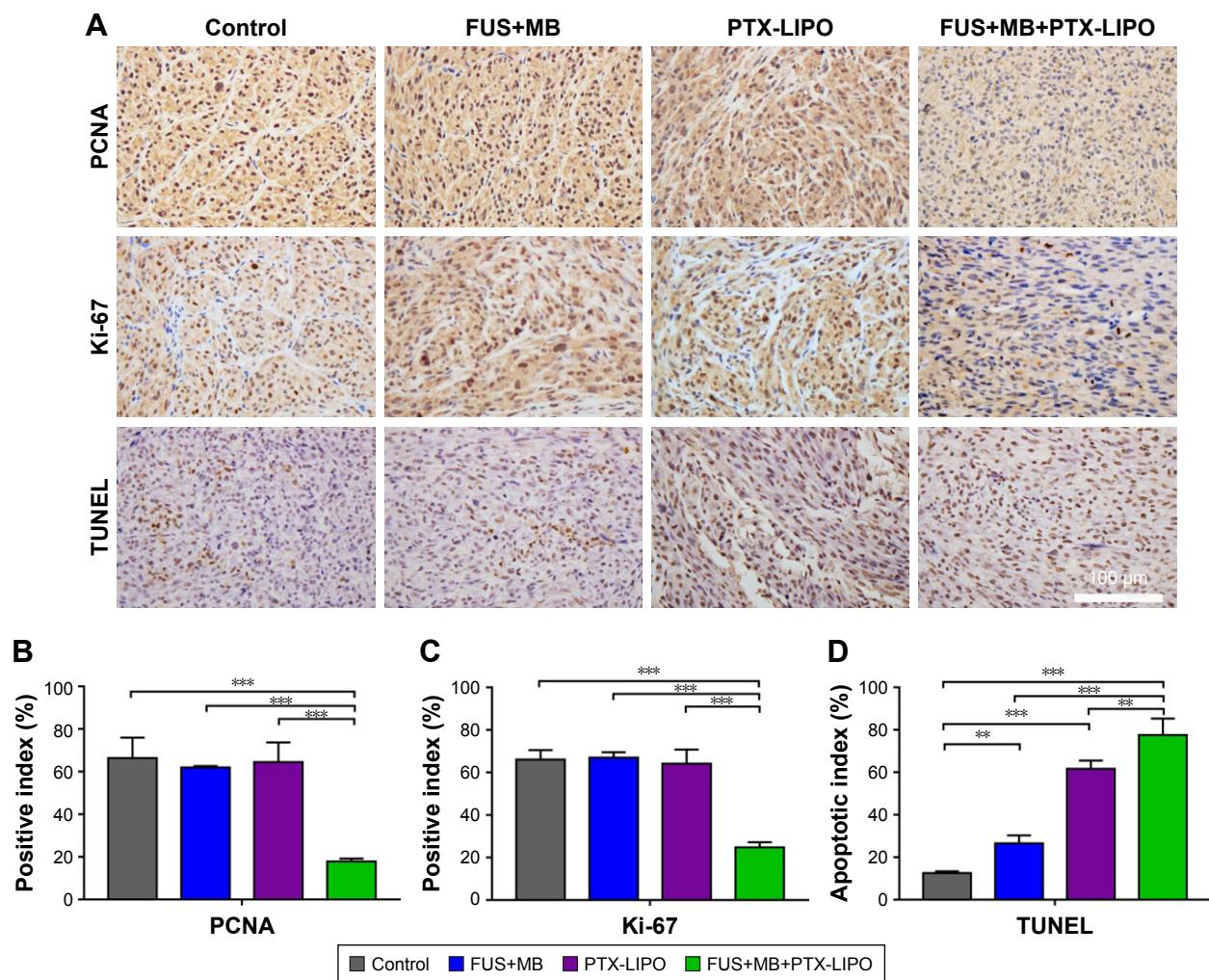
Figure 9 Proliferation and apoptosis analysis of glioblastoma in nude mice receiving different treatments: no treatment as the Control, FUS exposure with MBs but without PTX-LIPO as FUS+MB, PTX-LIPO injection only and PTX-LIPO delivery using FUS with MBs as FUS+MB+PTX-LIPO.
Notes: (**A**) Representative immunohistochemical staining of glioma sections against PCNA and Ki-67 and for the TUNEL assay. Cell nuclei were counterstained with hematoxylin. Glioma tissue was sampled 48 h after the treatment. Bar: 100 μm. Quantitative analysis of (**B**) PCNA-positive and (**C**) Ki-67-positive cells in the tumor region. The positive index was determined from the percentage of positive cells out of at least 2,000 tumor cells observed at 200× magnification. (**D**) Apoptosis quantification assessed by the percentage of TUNEL-positive cells in the glioma region. **P<0.01 and ***P<0.001.
Abbreviations: FUS, focused ultrasound; MBs, microbubbles; PTX-LIPO, paclitaxel liposomes; TUNEL, terminal dexynucleotidyl transferase-mediated dUTP nick end labeling.

Cell apoptosis in the glioma of nude mice in different treatment groups was also detected using the TUNEL assay. A small amount of apoptotic cells was observed in the control group, normally in the tumor center region, accounting for 12.5% in total (Figure 9A and D). When treated with PTX-LIPO and FUS+MB+PTX-LIPO, abundant TUNEL-positive cells appeared in the glioma region (Figure 9A). The quantitative results in Figure 9D show markedly elevated levels of apoptosis, increasing to 61.6% and 77.5% (P=0.0003). Additionally, treatment with FUS+MB alone also increased the apoptosis percentage to 26.5% (Figure 9D).

Discussion

PTX is a promising antineoplastic drug that has been proven to be effective against various extracranial cancers, such as

ovarian and breast cancer.[12,26] However, due to its poor water solubility, the commercial PTX preparation is formulated in polyethoxylated castor oil and dehydrated ethanol, and thus suffers from serious side effects, such as neurotoxicity and hypersensitivity reactions.[27] Among the various delivery systems under research and development, several liposomal PTX formulations have already been in different stages of clinical trials or even commercialized as therapies for several tumors, although not for brain tumors.[11] The BTB is the inevitable obstacle that must be overcome when using PTX liposomes as the chemotherapeutic agent for the treatment of brain tumors, especially glioblastoma.[28] Nonthermal bursts of FUS in the presence of circulating MBs has been demonstrated to open the BBB locally, noninvasively and reversibly in animal models ranging from large to small and

in nonhuman primates in the last decade.[5,7,10,29] Several unique advantages make this technology an attractive alternative approach for enhancing the delivery outcomes of various antitumor drugs, such as DOX, DOX-loaded liposomes, bevacizumab and temozolomide, crossing the BTB.[20,30–33] Hoping to take advantage of the existing liposomal agent, that is, without developing new drug formulations, and this promising drug delivery technique, we conducted this study and found that the results demonstrated for the first time that FUS combined with MBs could enhance the delivery outcome of PTX-LIPO in an in vivo intracranial glioblastoma murine model, significantly suppressing tumor growth and prolonging animal survival time.

Enhancing the drug accumulation dose in glioma is critical to improve chemotherapeutic efficacy. In this study, although PTX-LIPO injection alone produced a delaying effect on tumor progression to some extent, it did not significantly improve the survival time of the animals. Immunohistochemical analysis showed that the proliferation of glioma cells was still active, probably due to the low dose of extravasated drugs and despite the moderate increase in cell apoptosis. In contrast, the PTX concentration in glioma 1 h after delivering the drug using FUS with MBs could reach 1.85 µg/g of the tumor tissue, which was 3-fold higher than the amount that penetrated through leaky glioma vasculature itself. Furthermore, the concentration increased to 7.20 µg/g of the tumor tissue 3 h after treatment. In comparison to DOX-encapsulated liposomes delivered using FUS with MBs, which has been the most investigated liposomal drug in brain or brain tumor models, we found that the quantitative data in our study is comparable to the data obtained in other studies. Treat et al demonstrated that a therapeutically effective level of DOX (886±327 ng/g) could be achieved in normal rabbit brains using the systemic administration of Doxil (5.67 mg/kg) in conjunction with MRI-guided FUS with MBs (Optison, mean diameter: 2.0–4.5 µm, 0.1 mL/kg) to locally disrupt the BBB.[34] Most of the sonication parameters in their study (frequency: 1.7 MHz, pressure: 1.2 MPa, burst length: 10 ms, repetition frequency: 1 Hz and duration: 60–120 s) were similar with ours, except for the acoustic pressure, which was nearly 2-fold greater than the one used in this study. Moreover, their subsequent study showed that the DOX concentration reached 4.7 µg/g of the tumor tissue.[14,35] A strong tumor suppression effect was observed after three weekly treatments, while a single treatment induced a relatively modest increase of 24% in the median survival time of rats bearing 9L gliosarcoma.[15,16] In Yang et al's study, DOX liposomes radiolabeled with ^{111}In-oxine

(5 mg/kg) were prepared and delivered using 1.0 MHz FUS with a negative acoustic pressure of 0.7 MPa, PRF of 1 Hz and the duty cycle of 5%.[36] The DOX concentration in the sonicated glioma was determined to be 9 µg/g, which was 2-fold greater than that in unsonicated tumors. In addition, the median survival time of the glioblastoma-bearing mice was extended from 9 to 15 days.[37] Thus, the ameliorated therapeutic efficacy of nude mice bearing GBM in this study is largely attributable to the FUS-enhanced PTX-LIPO delivery efficiency.

In this study, PTX-LIPO was administered intravenously before sonication for the purpose of achieving a better delivery outcome. Our previous study showed a limited delivery efficiency of liposomes injected after sonication.[18] Aryal et al also found that the drug concentration could be significantly enhanced by nearly 50% when the drug was injected before sonication compared to the case of injection after sonication.[35] However, as a result of this, we did not know whether the PTX-LIPO structure was disrupted during sonication. We were also uncertain if PTX was still encapsulated or released to penetrate across the BTB. Although a few in vitro studies have shown that drugs could be released from liposomes when cavitation occurred during sonication and that sonication facilitated their uptake by cells, the case of an in vivo environment is a complex one that involves the MBs and liposomes circulating along with the blood in tiny microvessels.[38,39] It would, therefore, be necessary, yet challenging to further investigate the in vivo drug release mechanism facilitated by FUS with MBs.

Once the drugs cross the BTB through a route facilitated by FUS with MBs, they encounter a tumor microenvironment characterized by interstitial hypertension, which severely hinders the drug diffusion process. Studies have shown that drug delivery through the complex extracellular matrix mainly relies on passive diffusive transport, which is unfortunately inefficient for large particles.[40] Another study has shown that the interstitial diffusion coefficient of liposomes with a 75 nm hydrodynamic diameter in U87 MG cells growing in a cranial window was nearly one to two orders of magnitude lower than that of small molecules (<10 nm diameter).[41] By examining brain slices using fluorescence microscopy, it was also observed that the distribution pattern of fluorescently labeled liposomes penetrating the brain vasculature after BBB opening by FUS with MBs was heterogeneous with scattered spots, indicating confined diffusion in the extracellular matrix after extravasation from the microvasculature.[18] Thus, it is not yet known whether the penetration depth of drugs is sufficient to produce a therapeutic effect on tumor

cells far from the microvessels, once the drugs have crossed the disrupted BBB induced by FUS with MBs, and this is an important issue that requires further investigation.

In this study, we chose the U87 MG orthotopic glioblastoma model, which is widely used to mimic human GBM closely. In this study, the transplantation of U87 human glioma xenografts in nude Balb/c mice may provide the opportunity to assess the efficacy of the FUS-enhanced therapeutic strategy in human glioma. However, the immuno-deficiency of nude mice made the observation of the immune reactions against PTX-LIPO unavailable. Additionally, although this model is reproducible and actively angiogenetic, the tumors morphologically show well-demarcated growth patterns with narrow and diffuse infiltrative areas of tumor cells.[42–44] GBM is characterized by aggressive progression, diffuse infiltration into surrounding brain tissue and profuse neovascularization. In light of the fact that high infiltration is a crucial reason for the recurrence of GBM in patients after surgery, additional work on a more infiltrative model is needed to further investigate the augmentation of chemotherapeutic efficacy by FUS exposure in the presence of circulating MBs.

Several studies showed that pulsed ultrasound with MBs exerted influences on neurons. It has been reported that exposure of the hippocampus to pulsed FUS with MBs in Alzheimer's disease mice promoted neurogenesis in the dentate gyrus of the hippocampus based on the immunohistochemical analysis for doublecortin.[45] Such treatment also induced microglial activation revealed by decreased extent of branching and increased immunoreactivity for CD68, contributing to the internalization of plaques in microglial lysosomes.[46] Further investigation by Kovacs et al clearly demonstrated that pulsed FUS with MBs could induce the production of cytokines, chemokines and trophic factors linking to microglial activation.[47] Although our study focused on the therapeutic effect on the glioma cells, the effect of low-intensity FUS with MBs on healthy neurons near the tumors needs to be further investigated.

Conclusion

This study investigated the feasibility of enhancing the delivery of PTX-LIPO using pulsed low-intensity FUS exposure in the presence of circulating MBs as well as improving their therapeutic efficacy in an intracranial glioblastoma nude mice model. The results showed that FUS combined with MBs induced a significantly increased permeability of the BBB in vitro and BTB in vivo. Both qualitative and quantitative analyses proved that the accumulation of liposomes delivered by

this noninvasive approach in the glioblastoma was markedly enhanced, compared to the amount that penetrated through the leaky tumor vasculature. MRI longitudinal monitoring showed that intracranial glioblastoma progression was distinctly suppressed in nude mice treated with the enhanced PTX-LIPO chemotherapy facilitated by FUS with MBs. Meanwhile, the survival time of those nude mice was significantly prolonged. Immunohistochemical analysis further confirmed the antiproliferation effect and cell apoptosis induced by the enhanced PTX-LIPO delivery via FUS and MBs. These findings are expected to provide useful information for utilizing noninvasive low-intensity FUS with MBs as an effective strategy to deliver PTX-LIPO and improve their chemotherapeutic efficacy against glioblastoma.

Disclosure

The authors report no conflicts of interest in this work.

References

1. Stewart BW, Wild CP, editors. *World Cancer Report 2014*. 1st ed. Lyon, France: International Agency for Research on Cancer; 2014.
2. Pardridge WM. The blood–brain barrier: bottleneck in brain drug development. *NeuroRx*. 2005;2(1):3–14.
3. Bhowmik A, Khan R, Ghosh MK. Blood brain barrier: a challenge for effectual therapy of brain tumors. *Biomed Res Int*. 2015;2015: 320941.
4. Choi JJ, Pernot M, Small SA, Konofagou EE. Noninvasive, transcranial and localized opening of the blood-brain barrier using focused ultrasound in mice. *Ultrasound Med Biol*. 2007;33(1):95–104.
5. Hynynen K, McDannold N, Vykhodtseva N, Jolesz FA. Noninvasive MR imaging-guided focal opening of the blood-brain barrier in rabbits. *Radiology*. 2001;220(3):640–646.
6. Kinoshita M, McDannold N, Jolesz FA, Hynynen K. Noninvasive localized delivery of Herceptin to the mouse brain by MRI-guided focused ultrasound-induced blood-brain barrier disruption. *Proc Nat Aca Sci U S A*. 2006;103(31):11719–11723.
7. Marquet F, Teichert T, Wu SY, et al. Real-time, transcranial monitoring of safe blood-brain barrier opening in non-human primates. *PLoS One*. 2014;9(2):e84310.

8. McDannold N, Vykhodtseva N, Hynynen K. Blood-brain barrier disruption induced by focused ultrasound and circulating preformed microbubbles appears to be characterized by the mechanical index. *Ultrasound Med Biol*. 2008;34(5):834–840.

9. Shen YY, Zhang AL, Guo JX, Dan G, Chen SP, Yu H. Fluorescence imaging of Evans blue extravasation into mouse brain induced by low frequency ultrasound with microbubble. *Bio-Med Mater Eng*. 2014; 24(6):2831–2838.

10. McDannold N, Arvanitis CD, Vykhodtseva N, Livingstone MS. Temporary disruption of the blood-brain barrier by use of ultrasound and microbubbles: safety and efficacy evaluation in rhesus macaques. *Cancer Res*. 2012;72(14):3652–3663.

11. Surapaneni MS, Das SK, Das NG. Designing Paclitaxel drug delivery systems aimed at improved patient outcomes: current status and challenges. *ISRN Pharmacol*. 2012;2012:623139.

12. Singla AK, Garg A, Aggarwal D. Paclitaxel and its formulations. *Int J Pharm*. 2002;235(1–2):179–192.

13. Crosasso P, Ceruti M, Brusa P, Arpicco S, Dosio F, Cattel L. Preparation, characterization and properties of sterically stabilized paclitaxel-containing liposomes. *J Control Release*. 2000;63(1–2):19–30.

14. Aryal M, Park J, Vykhodtseva N, Zhang YZ, McDannold N. Enhancement in blood-tumor barrier permeability and delivery of liposomal doxorubicin using focused ultrasound and microbubbles: evaluation during tumor progression in a rat glioma model. *Phys Med Biol*. 2015; 60(6):2511–2527.

15. Treat LH, McDannold N, Zhang Y, Vykhodtseva N, Hynynen K. Improved anti-tumor effect of liposomal doxorubicin after targeted blood-brain barrier disruption by MRI-guided focused ultrasound in rat glioma. *Ultrasound Med Biol*. 2012;38(10):1716–1725.

16. Aryal M, Vykhodtseva N, Zhang YZ, Park J, McDannold N. Multiple treatments with liposomal doxorubicin and ultrasound-induced disruption of blood-tumor and blood-brain barriers improve outcomes in a rat glioma model. *J Control Release*. 2013;169(1–2):103–111.

17. Yan F, Li L, Deng Z, et al. Paclitaxel-liposome-microbubble complexes as ultrasound-triggered therapeutic drug delivery carriers. *J Control Release*. 2013;166(3):246–255.

18. Shen YY, Guo JX, Chen GS, et al. Delivery of liposomes with different sizes to mice brain after sonication by focused ultrasound in the presence of microbubbles. *Ultrasound Med Biol*. 2016;42(7):1499–1511.

19. Dehouck MP, Jolliet-Riant P, Brée F, Fruchart JC, Cecchelli R, Tillement JP. Drug transfer across the blood-brain barrier: correlation between in vitro and in vivo models. *J Neurochem*. 1992;58(5):8.

20. Aryal M, Arvanitis CD, Alexander PM, McDannold N. Ultrasound-mediated blood-brain barrier disruption for targeted drug delivery in the central nervous system. *Adv Drug Deliv Rev*. 2014;72:94–109.

21. Liu HL, Fan CH, Ting CY, Yeh CK. Combining microbubbles and ultrasound for drug delivery to brain tumors: current progress and overview. *Theranostics*. 2014;4(4):432–444.

22. Fan CH, Yeh CK. Microbubble-enhanced focused ultrasound-induced blood-brain barrier opening for local and transient drug delivery in central nervous system disease. *J Medical Ultrasound*. 2014;22(4):183–193.

23. Tomayko MM, Reynolds CP. Determination of subcutaneous tumor size in athymic (nude) mice. *Cancer Chemother Pharmacol*. 1989;24(3): 148–154.

24. Tung YS, Vlachos F, Choi JJ, Deffieux T, Selert K, Konofagou EE. In vivo transcranial cavitation threshold detection during ultrasound-induced blood-brain barrier opening in mice. *Phys Med Biol*. 2010;55(20): 6141–6155.

25. Zhan C, Lu W. The blood-brain/tumor barriers: challenges and chances for malignant gliomas targeted drug delivery. *Curr Pharm Biotechno*. 2012;13(12):2380–2387.

26. Kumar S, Mahdi H, Bryant C, Shah JP, Garg G, Munkarah A. Clinical trials and progress with paclitaxel in ovarian cancer. *Int J Women's Health*. 2010;2:411–427.

27. Koudelka S, Turanek J. Liposomal paclitaxel formulations. *J Control Release*. 2012;163(3):322–334.

28. Heimans JJ, Vermorken JB, Wolbers JG, et al. Paclitaxel (Taxol) concentrations in brain tumor tissue. *Ann Oncol*. 1994;5(10):951–953.

29. Huang Y, Alkins R, Schwartz ML, Hynynen K. Opening the blood-brain barrier with mr imaging-guided focused ultrasound: preclinical testing on a trans-human skull porcine model. *Radiology*. 2017;282(1): 123–130.

30. Boissenot T, Bordat A, Fattal E, Tsapis N. Ultrasound-triggered drug delivery for cancer treatment using drug delivery systems: from theoretical considerations to practical applications. *J Control Release*. 2016;241:144–163.

31. Liu HL, Hsu PH, Lin CY, et al. Focused ultrasound enhances central nervous system delivery of bevacizumab for malignant glioma treatment. *Radiology*. 2016;281(1):99–108.

32. Liu HL, Huang CY, Chen JY, Wang HY, Chen PY, Wei KC. Pharmacodynamic and therapeutic investigation of focused ultrasound-induced blood-brain barrier opening for enhanced temozolomide delivery in glioma treatment. *PLoS One*. 2014;9(12):e114311.

33. Fan CH, Cheng YH, Ting CY, et al. Ultrasound/magnetic targeting with SPIO-DOX-microbubble complex for image-guided drug delivery in brain tumors. *Theranostics*. 2016;6(10):1542–1556.

34. Treat LH, McDannold N, Vykhodtseva N, Zhang YZ, Tam K, Hynynen K. Targeted delivery of doxorubicin to the rat brain at therapeutic levels using MRI-guided focused ultrasound. *Int J Cancer*. 2007; 121(4):901–907.

35. Aryal M, Vykhodtseva N, Zhang YZ, McDannold N. Multiple sessions of liposomal doxorubicin delivery via focused ultrasound mediated blood-brain barrier disruption: a safety study. *J Control Release*. 2015; 204:60–69.

36. Yang FY, Wang HE, Liu RS, et al. Pharmacokinetic analysis of In-111-labeled liposomal doxorubicin in murine glioblastoma after blood-brain barrier disruption by focused ultrasound. *PLos One*. 2012; 7(9):e45468.

37. Yang FY, Wong TT, Teng MC, et al. Focused ultrasound and interleukin-4 receptor-targeted liposomal doxorubicin for enhanced targeted drug delivery and antitumor effect in glioblastoma multiforme. *J Control Release*. 2012;160(3):652–658.

38. Geers B, Lentacker I, Sanders NN, Demeester J, Meairs S, De Smedt SC. Self-assembled liposome-loaded microbubbles: the missing link for safe and efficient ultrasound triggered drug-delivery. *J Control Release*. 2011;152(2):249–256.

39. Afadzi M, Strand SP, Nilssen EA, et al. Mechanisms of the ultrasound-mediated intracellular delivery of liposomes and dextrans. *IEEE T Ultrason Ferr*. 2013;60(1):21–33.

40. Netti PA, Hamberg LM, Babich JW, et al. Enhancement of fluid filtration across tumor vessels: implication for delivery of macromolecules. *Proc Natl Acad Sci U S A*. 1999;96(6):3137–3142.

41. Pluen A, Boucher Y, Ramanujan S, et al. Role of tumor-host interactions in interstitial diffusion of macromolecules: cranial vs subcutaneous tumors. *Proc Natl Acad Sci U S A*. 2001;98(8):4628–4633.

42. Radaelli E, Ceruti R, Patton V, et al. Immunohistopathological and neuroimaging characterization of murine orthotopic xenograft models of glioblastoma multiforme recapitulating the most salient features of human disease. *Histol Histopathol*. 2009;24(7):879–891.

43. Jacobs VL, Valdes PA, Hickey WF, De Leo JA. Current review of in vivo GBM rodent models: emphasis on the CNS-1 tumour model. *ASN Neuro*. 2011;3(3):e00063.

44. Candolfi M, Curtin JF, Nichols WS, et al. Intracranial glioblastoma models in preclinical neuro-oncology: neuropathological characterization and tumor progression. *J Neuro-oncology*. 2007;85(2):133–148.

45. Burgess A, Dubey S, Yeung S, et al. Alzheimer disease in a mouse model: MR imaging-guided focused ultrasound targeted to the hippocampus opens the blood-brain barrier and improves pathologic abnormalities and behavior. *Radiology*. 2014;273(3):736–745.

46. Leinenga G, Gotz J. Scanning ultrasound removes amyloid-beta and restores memory in an Alzheimer's disease mouse model. *Sci Transl Med*. 2015;7(278):278ra33.

47. Kovacs ZI, Kim S, Jikaria N, et al. Disrupting the blood-brain barrier by focused ultrasound induces sterile inflammation. *Proc Natl Acad Sci U S A*. 2017;114(1):E75–E84.